Optical Materials: X 19 (2023) 100248

Contents lists available at ScienceDirect

Optical Materials: X

journal homepage: www.journals.elsevier.com/optical-materials-x

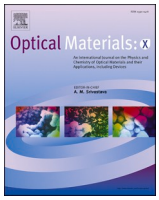

Er^{3+} doped tellurite whispering gallery mode microlasers in 1.5 μm–1.61 μm wavelength region generated by 0.98 μm and 1.48 μm pump lasers

Snigdha Thekke Thalakkal [a], Davor Ristić [a,*], Gualtiero Nunzi Conti [b], Stefano Pelli [b], Gabriele Frigenti [b], Hrvoje Gebavi [a], Alessandro Chiasera [c], Mile Ivanda [a]

[a] Institute Ruđer Bošković, Bijenička Cesta 54, 10000, Zagreb, Croatia
[b] IFAC-CNR Istituto di Fisica Applicata "Nello Carrara", Via Madonna del Piano 10, 50019, Sesto Fiorentino, FI, Italy
[c] IFN-CNR, CSMFO Lab. and FBK Photonics Unit, Via alla Cascata 56/C, 38123, Povo, TN, Italy

ARTICLE INFO

Keywords:
Whispering gallery modes
Er^{3+}
Microlaser
Tellurite

ABSTRACT

In this paper, we demonstrate Er^{3+} doped tellurite single and multi-mode microlasers in 1.5 μm–1.6 μm wavelength range fabricated via the plasma torch method. It is a simple and cost-effective method to produce microspheres with diameter ranges from 11 to 88 μm. Single mode laser output were observed with 0.98 μm and 1.48 μm pump, respectively. In addition, the quality factor of the fabricated microsphere is measured.

1. Introduction

Over the past two decades whispering gallery mode microcavities garnered considerable interest in many fundamental research areas including sensors, lasers, amplifiers and telecommunications [1–3]. Light in whispering gallery modes is spatially confined by total internal reflection along the equator of the microsphere resonators which makes these systems of interest appropriate for fiber optics and photonic applications. Distinctive properties of microspheres such as high quality factor and low mode volume makes them indispensable candidates for laser and telecommunication applications. The lasing properties of microsphere resonators have been widely reported in the literature over the past few years [4–6]. Glasses made of tellurite, phosphate, fluoride, and oxide glasses are desirable building blocks for microsphere lasers [7–11]. Glasses made up of these materials are effective hosts for rare earth ions which makes them suitable for lasing and telecommunication applications. As such, compared to other glasses, tellurite glass is a good host for rare earth ions because of its low phonon energy which leads to a broad and strong emission cross section. Moreover, their wide transparency window allows operation in the spectral range beyond 2 μm which enables the possibility of achieving longer wavelength generation compared to other glasses [9]. Possibilities of achieving longer wavelength generation in comparison with silica glasses by introducing rare earth ions such as Er^{3+}, Tm^{3+}, Ho^{3+}, Nd^{3+} and Yb^{3+} in tellurite host have led to a considerable increase in the production of tellurite glass microlasers [10–19]. The first report of tellurite glass microsphere production was reported in 2002 [10] using a two step method: first a tellurite glass rod was drawn from molten tellurite glass after which the tip of the rod was melted using a resistive heater. Because of surface tension the melted tip solidifies into a spherical shape. The two-step method described remains the most commonly used method to produce tellurite glass microspheres, where the final local heating can be done using a focused CO_2 laser [11–13], a resistive microheater [10,14] or a butane torch [15]. While the microspheres produced using the two-step method have the advantage of being attached to a fiber stem which is convenient for subsequent manipulation, the two-step method remains costly and time consuming since it includes an additional fiber drawing step. A simpler method is to produce the microspheres directly from powdered glass by melting individual glass powder grains, which was already reported using a focused Ti-saphire laser [16], a centrifugal spin-method [17] or by droping the powder through a vertical furnace [18]. In this paper, we used the plasma torch method to fabricate tellurite doped whispering gallery mode microspheres which is an effective and easy method for the fabrication of microspheres diameters ranging from 11 to 88 μm. While the plasma torch method was already used successfully to produce microspheres made of flouride glasses [20], in this paper we present the successful production of tellurite glass microspherical lasers using the plasma torch method. This makes possible the production of a large numbers of high-quality microsphere very quickly and using very affordable and cost-effective equipment.

* Corresponding author.
E-mail address: dristic@irb.hr (D. Ristić).

https://doi.org/10.1016/j.omx.2023.100248
Received 2 June 2023; Received in revised form 21 June 2023; Accepted 15 July 2023
Available online 19 July 2023

Er^{3+} doped tellurite microspheres have gained significant attention for broadband applications because of the possibility of achieving wavelength selective amplification. Recently, single mode and multimode laser generation of Er^{3+} doped tellurite microspheres was achieved in C-band and L-band under in-band pumping [14]. Furthermore, fiber taper coupled Er^{3+} doped microlasers at 1.5 μm region with 975 nm pump laser by novel spin method was reported [17]. Here, we report Er^{3+} doped tellurite whispering gallery mode microlaser using both by 980 nm and 1480 nm pumping.

2. Experimental

Er^{3+} doped tellurite microspheres were fabricated using the plasma torch method. $15Na_2O_25WO_360TeO_2$ glass doped with 0.5 mol% Er^{3+} powder is used for the fabrication of microspheres [22]. The glass is ground into a powder and then dropped between two electrodes through which an electrical discharge has been produced by applying a high AC voltage. Glass grains melt when passing through the electric arc and upon cooling acquire a spherical shape due to surface tension, after which they fall down on to a microscope slide. The distance between electrodes and microscopic slide is approximately 1 cm. Micrograph of the fabricated microspheres is shown in Fig. 1. A tapered fiber covered with UV curable glue is used to pick up the fabricated microsphere from the microscope slide (gluing process shown in Fig. 2 (a) and (b)). Fig. 3 shows the schematic of the plasma torch method used for the fabrication of Er^{3+} doped tellurite microspheres. Our experimental setup was realized with standard optical components spliced or connected using APC connectors. The pump lasers are multimode fiber coupled laser diodes at 980 nm (maximum power 600 mW) and 1480 nm (maximum power 200 mW) which are used to excite Er^{3+} ions in tellurite glass microspheres. The pump is connected through a multiplexer and a variable optical attenuator (VOA) to the input of the 95:5 coupler. The 95% splitter output is connected to the coupled microsphere system, while 5% of the coupler output is connected to a power meter.

A full tapered fiber made from standard SMF28 fiber was used to carry out the pumping of the microsphere and outcoupling of the generated radiation. The co-propagating light from the microsphere is analyzed using an optical spectrum analyzer (Anritsu MS9740B OSA). The schematic of experimental setup is shown in Fig. 4(a). Fig. 4(b) represents the micrograph of the green light upconversion in Er^{3+} doped tellurite microspheres. The green upconversion comes from the subsequent excited state absorption of: two photons in the case of 980 nm excitation ($^4I_{15/2}$->$^4I_{11/2}$->$^4F_{7/2}$); three photons in the case of 1480 nm excitation ($^4I_{15/2}$->$^4I_{13/2}$->$^4I_{9/2}$->$^4F_{7/2}$). Intense green up conversion

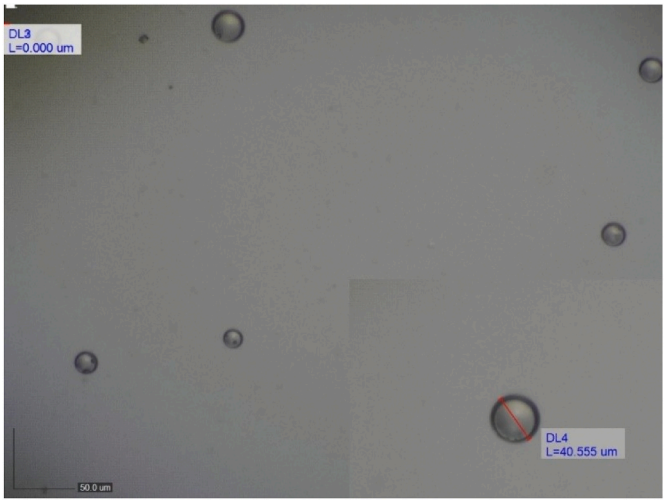

Fig. 1. Micrograph of fabricated Er^{3+} doped tellurite microsphere using the plasma torch method. The inset shows a microsphere with diameter 40.55 μm.

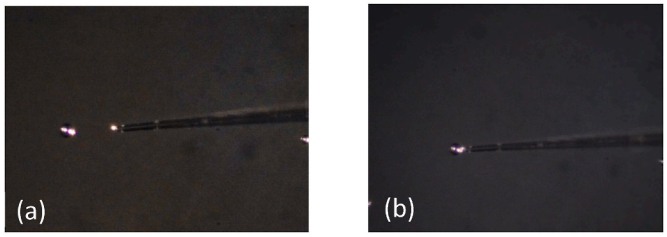

Fig. 2. (a) Micrographs of a tapered fiber and a microsphere in line with the tapered fiber. (b) Fabricated microsphere glued to the tip of the tapered fiber.

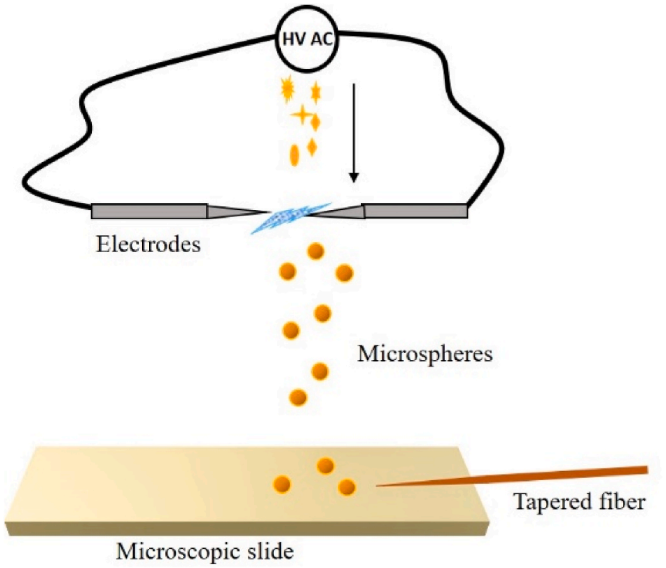

Fig. 3. schematic of plasma torch method used for the fabrication of Er^{3+} doped tellurite glass microspheres.

was always visible by eye in the case of both pump wavelengths and was used as an indication of efficient coupling. Furthermore, we measured the quality factor (Q) of the fabricated sphere. Fig. 5 depicts the experimental set up used for the Q factor measurement. Emission of a tunable laser is sent to the microsphere coupled to a standard silica-tapered fiber. Other end of the microsphere coupled system is connected to an InGaAs detector (Thorlabs DET08CFC/M). A sawtooth signal generator is used to detune the tunable laser. An oscilloscope syncronised to the signal generator is used to analyse the signal from the detector.

3. Results and discussion

The Er^{3+} ion has an absorption band at 980 nm. The simplified energy level diagram of Er^{3+} for optical pumping in 980 nm and 1480 nm wavelength is shown in the Fig. 6. 980 nm pump excites the ground state radiation from level $^4I_{15/2}$ to higher energy level $^4I_{11/2}$. In the case of tellurite glasses non-radiative transition from $^4I_{11/2}$ to $^4I_{13/2}$ is possible (2.7 μm). Subsequently, the level $^4I_{13/2}$ is populated, the transition from $^4I_{13/2}$ to $^4I_{15/2}$ takes place, and lasing is accomplished in 1.53 μm–1.6 μm range [9,17]. Hence, tellurite glasses are a good host for Er^{3+} to achieve lasing in 1.5 μm–1.6 μm wavelength region. Furthermore, in-band pumping is possible with 1480 nm pump and it is used to achieve laser emission at 1.5 μm. In our experiment we used 0.98 μm and 1.48 μm to obtain single and multimode lasing. Multimode lasing is observed beacuse many modes achieve lasing threshold condition. Fig. 7(a) shows the single mode lasing spectra with peak observed at 1558 nm with maximum laser intensity 23 nW using 980 nm pump. Fig. 7 (b) shows the

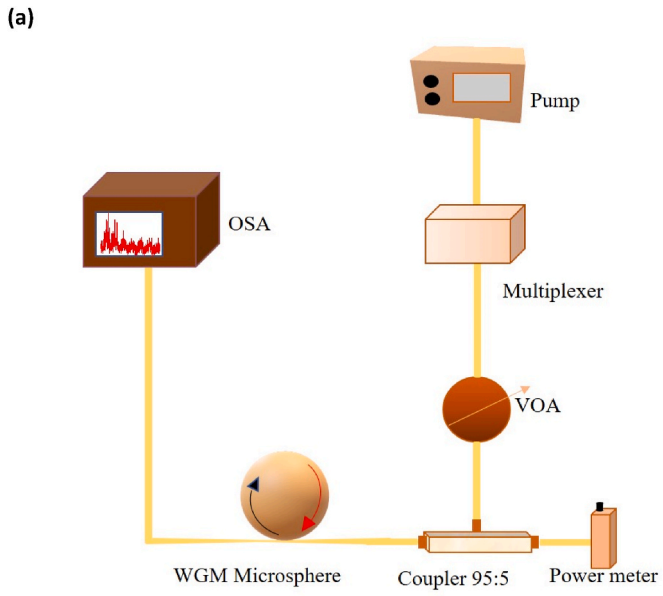

Fig. 4. (a) Schematic of the set up used for the Er^{3+} doped tellurite microsphere microlaser experiment (b) Green light up conversion observed with Er^{3+} doped tellurite microsphere while coupled to a full tapered fiber. (For interpretation of the references to colour in this figure legend, the reader is referred to the Web version of this article.)

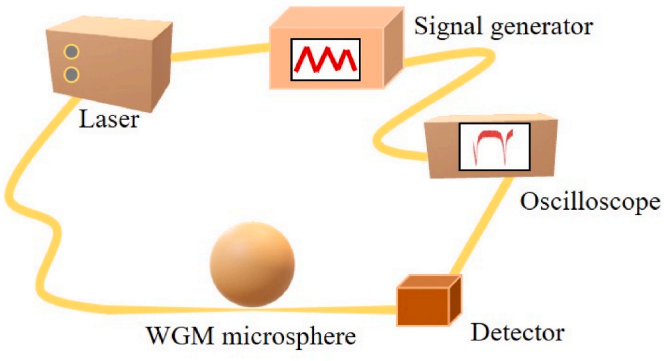

Fig. 5. Schematic diagram of the setup used for the Q factor measurement of Er^{3+} doped tellurite microspheres.

multimode lasing observed with 980 nm laser in the wavelength range 1560 nm–1600 nm. Fig. 8 (a) and (b) shows the multi mode lasing in 1590 nm–1610 nm range and single mode lasing of Er^{3+} doped tellurite microspheres achieved at 1565.41 nm with 1480 nm pump laser

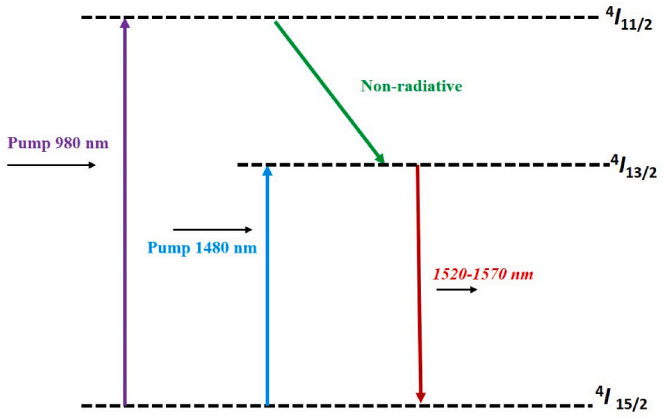

Fig. 6. Simplified Energy levels diagram of Er^{3+} doped tellurite glass for optical pumping in 980 nm and 1480 nm wavelength bands.

respectively. We can generate single and multimode lasing in Er^{3+} doped tellurite microsphere by adjusting the coupling strength by varying the contact position between the tapered fiber and the microsphere.

The measured laser output power versus absorbed pump power using 1.48 μm and 0.98 μm pump is shown in the Figs. 9 and 10 respectively. We examined the lasing intensity of the mode at the far end of the L-band (1600 nm) while increasing the pump power using a 1.48 μm laser in order to determine the lasing threshold. We confirmed that lasing output power is linearly increasing with the pump power. The lasing threshold is calculated for 1.48 μm and 0.98 μm pump lasers by linear fitting the laser output power in respect to the pump power. From the experiments we observed that the lasing threshold for 0.98 μm pump is greater than 1.48 μm pump. Calculated value of lasing threshold for mode at 1600 nm using 1.48 μm and 0.98 μm pump lasers are 12 mW and 16.58 mW respectively. Note that the threshold powers reported above all correspond to the pump power that is injected into the fiber taper that is used to couple the pump into the sphere and not to the power that is coupled into the sphere itself. The actual pump power coupled into the sphere is actually much lower than the power injected into the taper, however it is difficult to estimate how much exactly.

When the pump power is increased, the lasing mode is shifting to higher wavelengths. The observed mode shift from 1565.30 nm to 1566 nm is shown in the Fig. 11. The shifting range we observed is 0.7 nm. We hypothesize that the wavelength shift is due to the change of sphere size and refractive index [4,17,21]. From the equation (1), for the two consecutive modes,

$$2\pi n_{eff} R = m\lambda, \text{ m is an integer} \quad (1)$$

n_{eff} is the effective refractive index, R is the radius of the sphere, λ is the wavelength of the mode. The radius and refractive index together determine the wavelength of the whispering gallery modes according to equation (1). With increasing the pump power the temperature in the microsphere also increases. This subsequently alters the refractive index and radius of the microsphere. Hence, the effective optical path length changes which causes the shift of the wavelength of the lasing modes. For very low pump power, (just above the lasing threshold) we observed that the lasing mode is always located around 1.6 μm. Upon further increase of the pump power the modes around 1.6 stop lasing while the modes around 1565 μm start lasing. This is shown in Fig. 12 where we detected a peak at the far end of the L-band (1600.96 nm) for low pump powers while for higher pump powers we detected a lasing peak at lower wavelength (1566.77 nm). The absorption spectra at room temperature using a double beam spectrometer (resolution 1 nm) and the emission spectra at 1.5 μm for the glass composition we used is reported in Ref. [22]. The gain properties of the Er^{3+} doped tellurite glass determine

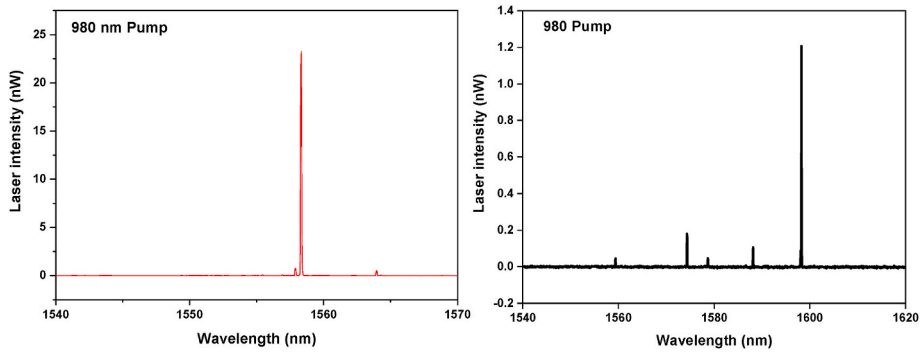

Fig. 7. (a) Single mode lasing spectra obtained at 1558 nm with maximum laser intensity 23 nW using 0.98 μm pump (b) Multimode lasing spectra obtained in the range 1560 nm–1600 nm using 0.98 μm pump.

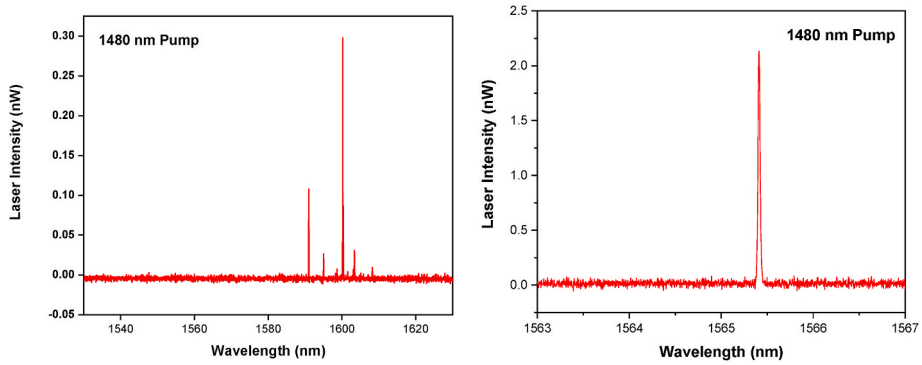

Fig. 8. (a) Multimode lasing observed in the range 1590 nm–1610 nm using 1.48 μm pump (b) Single mode lasing achevied at 1565.41 nm using 1.48 μm pump.

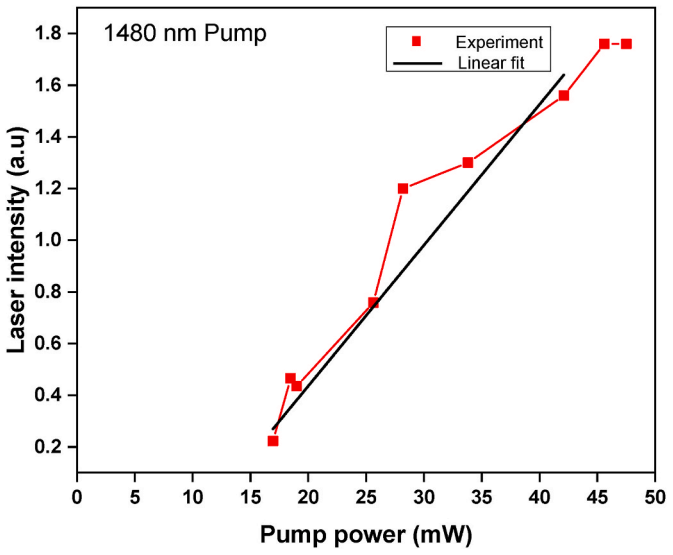

Fig. 9. Measured microsphere laser output versus absorbed pump power with 1.48 μm pump.

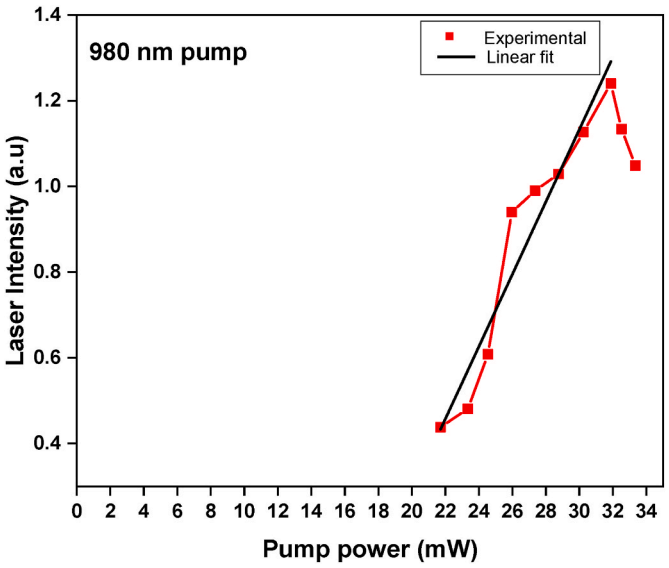

Fig. 10. Measured microsphere laser output versus absorbed pump power with 0.98 μm pump laser.

the L-band lasing wavelength of the microsphere laser. The ratio of absorption and emission cross-sections is crucial for determining the gain of the Er^{3+} doped tellurite glass for a given population inversion [17,21].

$$G \propto [\sigma_e(N_2/N) - \sigma_a(N_1/N)] \quad (2)$$

Where σ_e and σ_a are the emission and absorption cross section respectively, G is the gain, N is the Er^{3+} density of the tellurite glass, N_1 is the lower level population density and N_2 is the upper level population density. N_2/N is the inversion rate which is proportional to the pump power. Tellurite glass has a high refractive index, which results in a high emission cross section (σ_e) for Er^{3+} in tellurite glasses. The measured refractive index of the sample (WNT 05) used for the experiment is 2.0450 [22]. Moreover, the effective emission cross section bandwidth is very large in tellurite glasses. When the ratio N_2/N_1 is small, G is positive in the longer wavelength end of the L-band (1600.96 nm). We confirmed

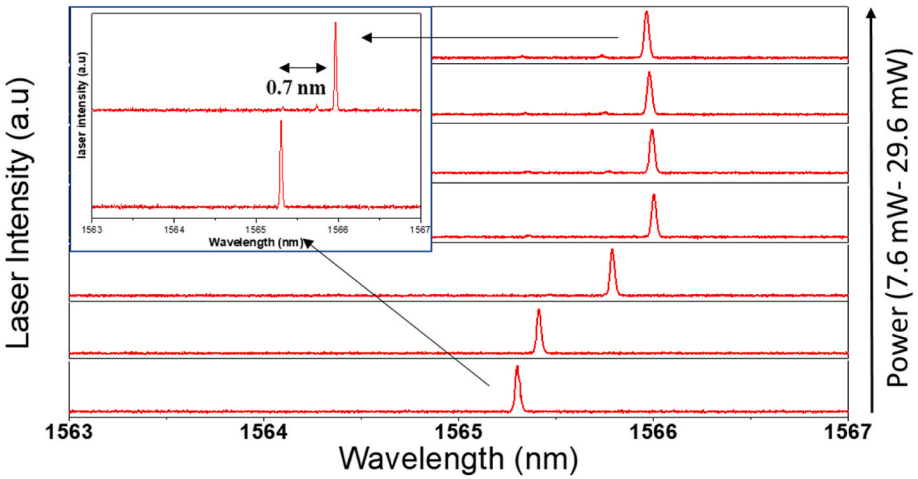

Fig. 11. Observed mode shift to longer wavelength region while increasing the 1.48 μm pump power. Inset represents the wavelength shift 0.7 nm achieved while increasing the pump power.

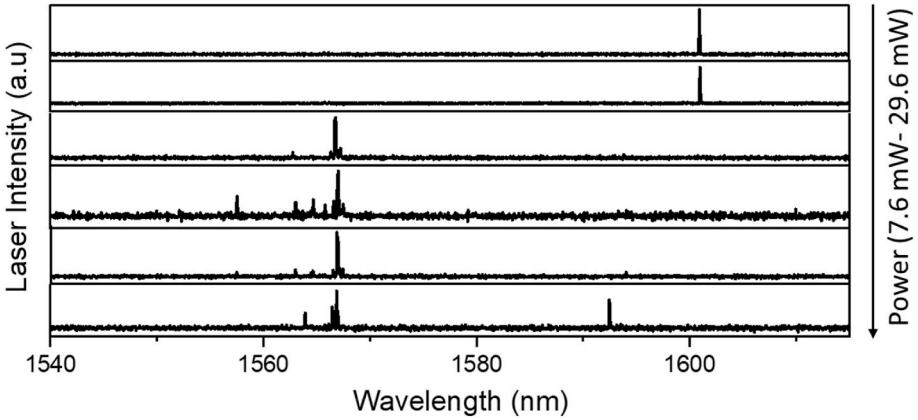

Fig. 12. Lasing mode at 1600 nm shifted to shorter wavelength while increasing the 1.48 μm pump power.

that the gain is positive in this region since we observed microspheres lasing in this region.

When increasing the pump power above a certain level the mode around 1600 nm stops lasing and the mode at 1565 nm starts lasing. This is because when increasing the pump power the inversion rate also increases, and then the gain become positive in the shorter wavelength region. Therefore, microsphere will lase in the shorter wavelength region (1566.77 nm) [17,21]. Although a further increase in the pump power and a consequential increase in the population inversion should lead to a further change of the preferred lasing wavelength down to 1530 nm where the maximum of Er^{3+} emission is located, in practice we have been unable to observe lasing at such low wavelengths. In fact, upon increasing the pump power we have found that the spheres tended to melt before full population inversion could be reached. When the pump power is increased, spheres with diameters less than 30 μm melt quickly. This is due to the fact that the breakdown temperature of a microsphere changes with size. The smaller the diameter, the easier it is to melt..

Furthermore, the quality factor of the microsphere is measured using the set up shown in Fig. 5. Q factor is calculated by Lorenz fitting to a whispering gallery mode measured at 1.63 μm wavelength (Fig. 13) where we expect the absorption of the Er^{3+} ions to be minimal. The full width at half maxima of the fitted peak is 134.59 MHz (shown in the inset of Fig. 13) and the calculated value of the Q factor is 1.36×10^6.

Table 1
Parameters after the Lorentz fitting of the Q factor measurement.

Model	Lorentz
Equation	y = y0 + (2*A/pi)*(w/(4*(x-xc)^2 + w^2))
Plot	of
y0	174.93487 ± 0.77047
xc	6964.27456 ± 3.0173
w	134.59019 ± 9.71079
A	−16193.61337 ± 934.51514
Reduced Chi-Sqr	74.2134
R-Square (COD)	0.79271
Adj. R-Square	0.78964

4. Conclusion

In conclusion, we have reported Er^{3+} doped tellurite glass microsphere single and multimode lasers generated by pump lasers at 1.48 μm and 0.98 μm wavelength using a home made plasma torch. The suggested plasma torch approach is used to fabricate microspheres with diameters 11–88 μm simultaneously. With a 0.98 μm as pump laser, we were able to achieve a 23 nw single mode laser. The lasing threshold for 1.48 μm pump is 12 mW which is less than the measured value of the lasing threshold for 0.98 μm pump (16.58 mW). When the 1.48 μm pump laser power is increasing, the lasing peak at 1565.30 nm shifts to a higher wavelength region because of cavity length changes due to heat deposition in the microsphere. In addition, we studied the preferred

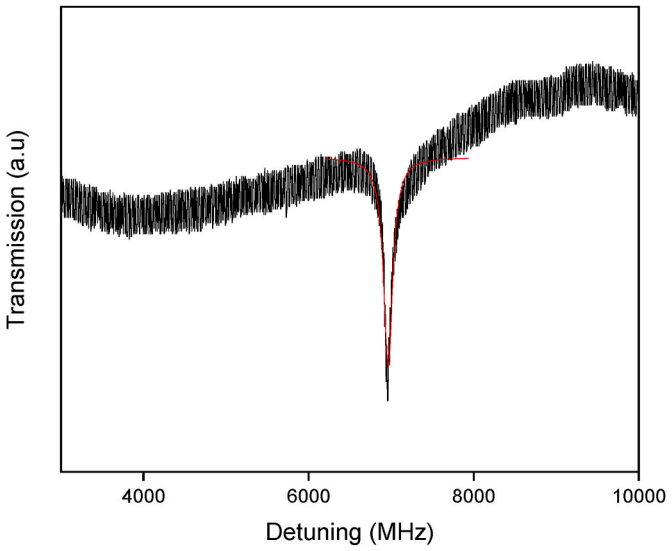

Fig. 13. Lorenz fitting of the transmittance of the fabricated microsphere laser for the Q factor measurement. Table 1 shows the parameters after fitting.

lasing wavelength in the L -band by observing peaks at 1.6 μm and 1565 nm, and we found that both can lase depending on the inversion dependent positive net cross section in the shorter wavelength region. The measured value of the Q factor of the fabricated microspheres in this work reaches 1.36×10^6.

CRediT authorship contribution statement

Snigdha Thekke Thalakkal: Conceptualization, Methodology, Investigation, Validation, Writing – original draft. **Davor Ristić:** Conceptualization, Methodology, Validation, Writing – review & editing, Supervision, Project administration, Funding acquisition. **Gualtiero Nunzi Conti:** Writing – review & editing, Resources. **Stefano Pelli:** Writing – review & editing, Resources. **Gabriele Frigenti:** Resources. **Hrvoje Gebavi:** Methodology, Resources. **Alessandro Chiasera:** Writing – review & editing. **Mile Ivanda:** Writing – review & editing, Project administration, Funding acquisition.

Declaration of competing interest

The authors declare that they have no known competing financial interests or personal relationships that could have appeared to influence the work reported in this paper.

Data availability

Data will be made available on request.

Acknowledgment

Croatian Science Foundation IP-2019-04-3045; Croatian Government and the European Union through the European Regional and Development Fund - the Competitiveness and Cohesion Operational Programme (KK.01.1.1.01.0001). We thankfully acknowledge Prof. Adolfo Speghini, University of Verona, for providing tellurite glass samples.

References

[1] K.J. Vahala, Optical microcavities, Nature 424 (2003) 839–846, https://doi.org/10.1038/nature01939.
[2] A. Chiasera, Y. Dumeige, P. Féron, M. Ferrari, Y. Jestin, G. Nunzi Conti, S. Pelli, S. Soria, G.C. Righini, Spherical whispering-gallery-mode microresonators, Laser Photon. Rev. 4 (3) (2010) 457–482, https://doi.org/10.1002/lpor.200910016.
[3] V.S. Ilchenko, A.B. Matsko, Optical resonators with whispering-gallery modes—part II: applications, IEEE J. Sel. Top. Quant. Electron. 12 (2006) 15–32, https://doi.org/10.1109/JSTQE.2005.862943.
[4] F. Lissillour, D. Messager, G. Stéphan, P. Féron, Whispering-gallery-mode laser at 1.56 μm excited by a fiber taper, Opt Lett. 26 (14) (2001) 1051–1053, https://doi.org/10.1364/OL.26.001051.
[5] J. Kalkman, A. Polman, T.J. Kippenberg, K.J. Vahala, Mark L. Brongersma, Erbium-implanted silica microsphere laser, Nucl. Instrum. Methods Phys. Res. Sect. B Beam Interact. Mater. Atoms 242 (1–2) (2006) 182–185, https://doi.org/10.1016/j.nimb.2005.08.160.
[6] J. Yu, X. Wang, W. Li, M. Zhange, J. Zhang, K. Tian, Y. Du, S.N. Chormaic, P. Wang, An experimental and theoretical investigation of a 2 μm wavelength low-threshold microsphere laser, J. Lightwave Technol. 38 (7) (2020) 1880–1886, https://doi.org/10.1109/JLT.2019.2958349.
[7] P. Feron, Whispering gallery mode lasers in erbium doped fluoride glasses, Ann. Fond. Louis Broglie 29 (2004) 1–2.
[8] C.H. Dong, Y. Yang, Y.L. Shen, C.L. Zou, F.W. Sun, H. Ming, G.C. Guo, Z.F. Han, Observation of microlaser with Er-doped phosphate glass coated microsphere pumped by 780 nm, Opt Commun. 283 (24) (2010) 5117–5120, https://doi.org/10.1016/j.optcom.2010.07.018.
[9] E.A. Anashkina, Laser sources based on rare-earth ion doped tellurite glass fibers and microspheres, Fibers 8 (5) (2020) 30, https://doi.org/10.3390/fib8050030.
[10] K. Sasagawa, K. Kusawake, J. Ohta, M. Nunoshita, Nd-doped tellurite glass microsphere laser, Electron. Lett. 38 (22) (2002) 1355–1357, https://doi.org/10.1049/EL%3A20020929.
[11] A. Li, Y. Dong, S. Wang, S. Jia, G. Brambilla, P. Wang, Infrared-laser and upconversion luminescence in Ho^{3+}-Yb^{3+} codoped tellurite glass microsphere, J. Lumin. 218 (2020), 116826, https://doi.org/10.1016/j.jlumin.2019.116826.
[12] S. Kang, T. Ouyang, D. Yang, Q. Pan, J. Qiu, G. Dong, Enhanced 2 μm mid-infrared laser output from Tm3+-activated glass ceramic microcavities, Laser Photon. Rev. 14 (2020), 1900396, https://doi.org/10.1002/lpor.201900396.
[13] F. Vanier, F. Côté, M.E. Amraoui, Y. Messaddeq, Y. Peter, M. Rochette, Low-threshold lasing at 1975 nm in thulium-doped tellurite glass microspheres, Opt. Lett. 40 (2015) 5227–5230.
[14] E.A. Anashkina, A.V. Andrianov, Erbium-doped tellurite glass microlaser in C-band and L-band, J. Lightwave Technol. 39 (11) (2021) 3568–3574, https://doi.org/10.1109/JLT.2021.3064999.
[15] J. Qin, Y. Huang, T. Liao, C. Xu, C. Ke, Y. Duan, 1.9 μm laser and visible light emissions in Er3+/Tm3+ co-doped tellurite glass microspheres pumped by a broadband amplified spontaneous emission source, J. Opt. 21 (2019), 035401, https://doi.org/10.1088/2040-8986/ab0264.
[16] T. Kishi, T. Kumagai, S. Shibuya, F. Prudenzano, T. Yano, S. Shibata, Quasi-single mode laser output from a terrace structure added on a Nd3+-doped tellurite-glass microsphere prepared using localized laser heating, Opt Express 23 (2015) 20629–20635, https://doi.org/10.1364/OE.23.020629.
[17] X. Peng, F. Song, S. Jiang, M. Gonokami, N. Peyghambarian, Fiber-taper-coupled L-band Er^{3+}-doped tellurite glass microsphere laser, Appl. Phys. Lett. 82 (10) (2003) 1497–1499, https://doi.org/10.1117/12.474768.
[18] Z. Yang, Y. Wu, K. Yang, P. Xu, W. Zhang, S. Dai, T. Xu, Fabrication and characterization of Tm3+-Ho3+ co-doped tellurite glass microsphere lasers operating at ~2.1 μm, Opt. Mater. 72 (2017) 524–528, https://doi.org/10.1016/j.optmat.2017.06.057.
[19] J. Wu, S. Jiang, T. Qua, M.K. Gonokami, N. Peyghambarian, 2 μ m lasing from highly thulium doped tellurite glass microsphere, Appl. Phys. Lett. 87 (21) (2005), 211118, https://doi.org/10.1063/1.2132532.
[20] F. Lissillour, K. Äit-Ameur, N. Dubreuil, G. Stephan, M. Poulain, Whispering-gallery mode Nd-ZBLAN microlasers at 1.05 μm, SPIEL 3416 (1998) 150, https://doi.org/10.1117/12.323384.
[21] P.C. Becker, N.A. Olsson, J.R. Simpson, Erbium-doped Fiber Amplifiers—Fundamentals and Technology, Academic Press, 1999.
[22] G.N. Conti, V.K. Tikhomirov, M. Bettinelli, S. Berneschi, M. Brenci, B. Chen, S. Pelli, A. Speghini, A.B. Seddon, G.C. Righini, Characterization of ion-exchanged waveguides in tungsten tellurite and zinc tellurite Er^{3+}-doped glasses, Opt. Eng. 42 (10) (2003) 2805–2811, https://doi.org/10.1117/1.1604782.